

Chasing Lipids in Health and Diseases by CARS Microscopy

Ji-Xin Cheng*, Haifeng Wang, Thuc T. Le, Yan Fu, Terry B. Huff, Han-Wei Wang

Weldon School of Biomedical Engineering and Department of Chemistry,
Purdue University, West Lafayette, IN 47907, USA

Abstract

The integration of near IR picosecond pulse excitation, collinear beam geometry, epi-detection, and laser-scanning has produced a coherent anti-Stokes Raman scattering (CARS) microscope with a detection sensitivity of 10^5 vibrational oscillators, sub-micron 3D resolution, and video-rate acquisition speed. The incorporation of spectral detection and other imaging modalities has added versatility to the CARS microscope. CARS microscopy is a sensitive imaging tool of lipids that have a high density of CH_2 group. Initial works have shown its great potential in the study of demyelinating diseases, obesity, and cardiovascular diseases. CARS microscopy is poised to become a powerful bio-imaging tool with the availability of a multifunctional, affordable, easy-to-operate CARS microscope, and the development of CARS endoscopy for in vivo diagnosis.

1. Introduction

Coherent anti-Stokes Raman scattering (CARS) microscopy is a nonlinear optical imaging technique that allows high-speed vibrational imaging of molecules. In a CARS process, three laser fields at the pump (ω_p), Stokes (ω_s), and probe (ω'_p) frequencies interact with a medium to generate a new field at the anti-Stokes frequency $\omega_{as} = (\omega_p - \omega_s) + \omega'_p$. In most experiments, the pump field E_p and probe field E'_p come from the same laser beam. When the beating frequency ($\omega_p - \omega_s$) is in resonance with a molecular vibration, the mixed pump and Stokes field can effectively excite the molecule to a vibrational state.¹ The efficiency of CARS is then significantly enhanced because the molecular vibration facilitates the energy exchange between light fields. Therefore, the molecules in resonance will show higher signal than those off resonance, providing a vibrational contrast in a CARS image. On the other hand, without vibrational resonance CARS can still happen through electronic motions, which produces the nonresonant background. As a formal description, the CARS signal arises from the third-order induced polarization, $P^{(3)} = \chi^{(3)} E_p E_s^* E'_p$, where the susceptibility $\chi^{(3)}$ has a nonresonant component and a Raman resonant component. Because of the interference between the resonant and nonresonant components, the CARS spectrum is dispersed comparing with the spontaneous Raman spectrum, with a shift of the peak to lower frequency and appearance of a dip at higher frequency.¹ CARS microscopy offers several unique advantages.

- CARS imaging is non-destructive so that it can be applied to live animals and tissues.
- As a coherent process, the CARS fields from different molecules have a well defined phase relationship and they add up like the emission from an antenna array. The emission is concentrated in one direction defined by the constructive interference, which greatly facilitates the signal collection. The coherent addition also results in a quadratic signal increase with respect to the density of molecular oscillators, versus the linear increase of spontaneous Raman signal. For a bulk liquid, the CARS signal is larger than the spontaneous Raman signal by 9 orders of magnitude.¹ Therefore a CARS image can be acquired in one second or less while a confocal Raman image may take hours.

- CARS signal appears at a wavelength shorter than the excitation wavelengths, spectrally separated from the one-photon fluorescence background that Raman microscopy suffers from.
- The nonlinear dependence on excitation intensity ensures that the CARS signal is only generated in the focal center, providing an inherent sub-micron 3D spatial resolution good for studying single cells.

The major disadvantage of CARS is the existence of the nonresonant background which limits the sensitivity in detecting weak Raman bands. In the past few years, various methods have been developed for suppressing the nonresonant background and pushing the detection sensitivity, making CARS microscopy a mature imaging technique for biological applications, especially for chasing the roles of lipids in health and diseases.

In a traditional view, lipids serve as structural components of membranes, energy storage, and hormones. Recent studies of membrane microdomains have revealed important roles of lipids in signal transduction and membrane trafficking in cells.² Lipids contribute up to 70% dry weight of the central nervous system in the form of myelin sheath, while the etiology of many demyelinating diseases such as multiple sclerosis remains elusive. The significance of lipids to health has dramatically increased with obesity reaching an epidemic proportion in the United States. Because the Raman-resonance enhancement of $\chi^{(3)}$ is significant due to the high density of C-H bonds in lipid molecules, CARS is a naturally sensitive imaging tool for lipids. Li *et al.* have demonstrated the sensitivity of selectively probing 20,000 lipid molecules inside the focal area with epi-detected CARS.³

This article reviews recent applications of CARS microscopy to lipid-related diseases. The rest of the paper is organized as follows. Section 2 presents the development of a state-of-the-art CARS microscope. Section 3 describes the application of CARS microscopy to white matter imaging and demyelination diseases. Section 4 describes the study of obesity associated health risks. Section 5 presents an outlook.

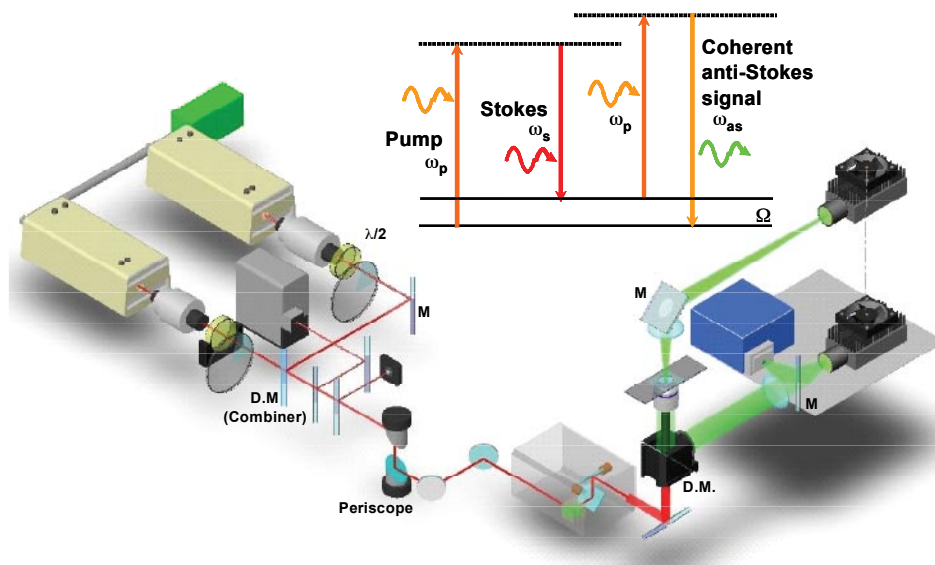


Figure 1. Schematic of a laser-scanning CARS microscope that allows imaging with forward-detected CARS (F-CARS), epi-detected CARS (E-CARS), two-photon excitation fluorescence (TPEF), and sum frequency generation (SFG) signals produced by two synchronized pulsed lasers at frequencies ω_p and ω_s . The energy diagram of CARS is shown above the setup. M.: Mirror; D.M.: Dichroic Mirror

2. A state-of-the-art CARS Microscope

The first CARS microscope was made by Duncan and coworkers in 1982 using a non-collinear beam geometry⁴ based on the conventional wisdoms from CARS spectroscopy. CARS microscopy was revived by Xie and coworkers in 1999 using a collinear beam geometry under the tight focusing condition.⁵ In the past several years, significant advances in instrumentation have resulted in a robust CARS microscope as shown in Fig. 1. The key features are:

Near IR laser excitation. Near IR lasers first used by Zumbusch et al. for CARS imaging avoids two-photon electronic enhancement of the nonresonant background,⁵ reduces the photodamage induced by multiphoton absorption,⁶ and diminishes tissue scattering leading to increased optical penetration depth.⁷

Picosecond pulse excitation. Femtosecond pulses are generally used in nonlinear optical (NLO) imaging for the high peak power. However, the spectral width of a femtosecond pulse is much broader than the width of most Raman lines, therefore most of the energy does not couple with molecular vibration but contributes to the nonresonant background. Instead, the spectral width of a picosecond pulse matches the Raman line width, so that the excitation energy can be focused on a single Raman band to provide good spectral resolution and excellent vibrational contrast.⁸

Collinear beam geometry. Non-collinear beam geometry was used in CARS spectroscopy to fulfill the phase matching condition. When the interaction length became very small ($\sim 1 \mu\text{m}$) under the tight focusing condition in microscopy, the phase matching condition could be fulfilled with a collinear beam geometry for forward-detected CARS (F-CARS).⁵ The collinear beam geometry greatly simplified the optical alignment and has been a key step in producing high-quality CARS images.

Epi- (i.e., backward-) detection. For objects smaller than the excitation wavelengths, the phase matching condition was fulfilled in both forward and backward direction.⁹ Systematic study showed that epi-detected CARS (E-CARS) could arise from small objects,

discontinuity of $\chi^{(3)}$ at an interface, and back-reflection of forward CARS.ard CARS.¹⁴ Because the CARS signal from a bulk medium goes forward, E-CARS provides an effective way to detect small objects.⁹ E-CARS is also important for live animal imaging where the F-CARS signal cannot pass through a thick tissue.^{10, 11}

Laser-scanning. High-sensitivity imaging was achieved by scanning picosecond lasers of high repetition rates (in MHz), with an image acquisition speed of a frame per second¹² or video rate.¹⁰

Multimodality. Multimodality is important because different NLO imaging methods have their distinctive advantages: two-photon excitation fluorescence (TPEF) can be used to visualize proteins, ions with fluorescent labeling or specific autofluorescent structures; sum-frequency generation (SFG) is selective to non-centrosymmetric molecular assemblies such as collagen fibrils; CARS is naturally sensitive to lipid-enriched structures such as adipocytes. The two picosecond laser beams for CARS could also be used for electronic SFG. Fu et al. demonstrated multimodal NLO imaging of ex vivo spinal tissues by CARS imaging of myelin sheath, SFG imaging of astrocyte processes, and TPEF imaging of calcium indicators on the same platform.¹³

In summary, a combination of the above strategies has produced a CARS microscope with high detection sensitivity, high imaging speed, and multi-channel information. Two applications of CARS microscopy to lipid related health risks are shown below.

3. CARS Imaging of Intact Myelin Sheath to Elucidate Demyelination Mechanism

Myelin sheath is a multiple-layer membrane (Fig. 2A) wrapping the long extensions of neurons called axons.¹⁴ The myelin sheath is interrupted at intervals called the nodes of Ranvier which are rich in sodium channels. This organization makes the nerve impulses move in a stepwise fashion called "saltatory conduction". Being of high resistance, myelin is crucial for the high saltatory

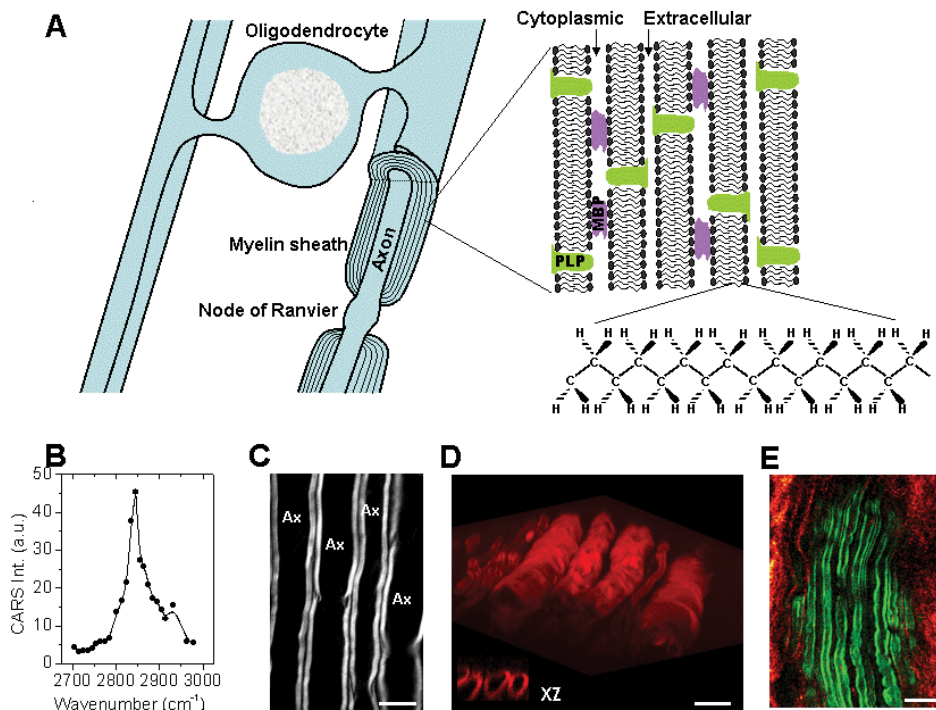


Figure 2. (A) Diagram shows the myelin sheath in the central nervous system. The myelin is a multiple-layer membrane formed by oligodendrocytes, containing a high lipid to protein ratio. MBP: myelin basic protein. PLP: proteolipid protein. (B) E-CARS spectrum of a single axonal myelin sheath measured by manually tuning the Stokes laser wavelength. The pump laser frequency was fixed at 14081 cm^{-1} . (C) E-CARS image of myelin sheath wrapping around the axons when the Raman shift was tuned to 2840 cm^{-1} . Bar = $10\text{ }\mu\text{m}$. (D) Reconstruction of 3D CARS imaging of myelin sheath in spinal tissue. The inset is XZ images showing the transverse section of myelin sheath. Bar = $10\text{ }\mu\text{m}$. (E) *In vivo* E-CARS imaging of myelinated axons and SHG imaging of collagen fibrils surrounding sciatic nerve and between the axons. Bar = $20\text{ }\mu\text{m}$.

conduction speed. Numerous neurological diseases specifically attack the myelin sheath causing demyelination with disabling and often fatal results. The most common demyelination disease is multiple sclerosis affecting the 2.5 million people worldwide. The lamellar structure of myelin sheath has been well characterized by polarized light microscopy, electron microscopy, and X-ray diffraction. However, these techniques necessitate fixed tissues which prevent the examination of cellular activities in real time. Magnetic resonance imaging is used for *in vivo* imaging of white matter, but its resolution is too poor for single cell observation.

The myelin contains about 70% lipid and 30% protein by weight. The high density of CH_2 groups in the myelin membrane (Fig. 2A) leads to a large and directional CARS signal, making CARS microscopy a sensitive tool for imaging myelin sheath in its natural state. Using the resonant CARS signal from CH_2 , our group has performed a systematic imaging study of intact neuronal myelin in *ex vivo* tissues¹⁵ and live animals.¹¹ The sample used in our *ex vivo* study is the spinal cord white matter isolated from guinea pigs. The tissue was kept in the oxygen-bubbled Krebs' solution. Fig. 2B shows an E-CARS spectrum of a single axonal myelin. The peak for the symmetric CH_2 stretch vibration appears at 2840 cm^{-1} , with a resonant signal to nonresonant background ratio of 10:1. High CARS contrast of parallel myelin wrapping around the axons was shown in Fig. 2C. With a lateral resolution of $0.28\text{ }\mu\text{m}$ and an axial resolution of $0.70\text{ }\mu\text{m}$, we were able to probe the detailed myelin structures such as the paranodal myelin.¹⁵ Moreover, the inherent

3D resolution allowed us to visualize the 3D organization of myelin tubes (Fig. 2D).

Recently our group has applied laser-scanning CARS microscopy to *in vivo* imaging of deep tissues.¹¹ *In vivo* imaging is crucial to the study of biological systems under the most natural condition. The label-free advantage of CARS is particularly important for *in vivo* studies where the labeling is complicated by inefficient diffusion and non-specific binding. By using minimal surgery to cut open the skin, Huff et al. demonstrated *in vivo* E-CARS imaging of sciatic nerve and surrounding adipocytes.¹¹ The *in vivo* E-CARS signal could arise from interfaces as well as back scattering of forward CARS signal. Fig. 2E shows the E-CARS image of myelin sheath and second harmonic generation image of collagen fibrils around the sciatic nerve in a live mouse

The capability of imaging myelin in its natural state allowed us to investigate the mechanisms of demyelination which are still poorly understood. The demyelination model we have studied is lysophosphatidylcholine (lyso-PtdCho) induced acute myelin vesiculation.¹⁶ After injection of lyso-PtdCho into the spinal tissue, we observed extensive and acute myelin degradation which was characterized by decrease of CARS intensity (Fig. 3A-C) and loss of dependence on excitation polarization (Fig. 3D-F). The loss of lamellar structure and reduction of packing density correspond to myelin vesiculation observed by electron microscopy. With these capabilities, we have examined the enzymatic activities involved in lyso-PtdCho induced myelin degradation. The degradation lesion

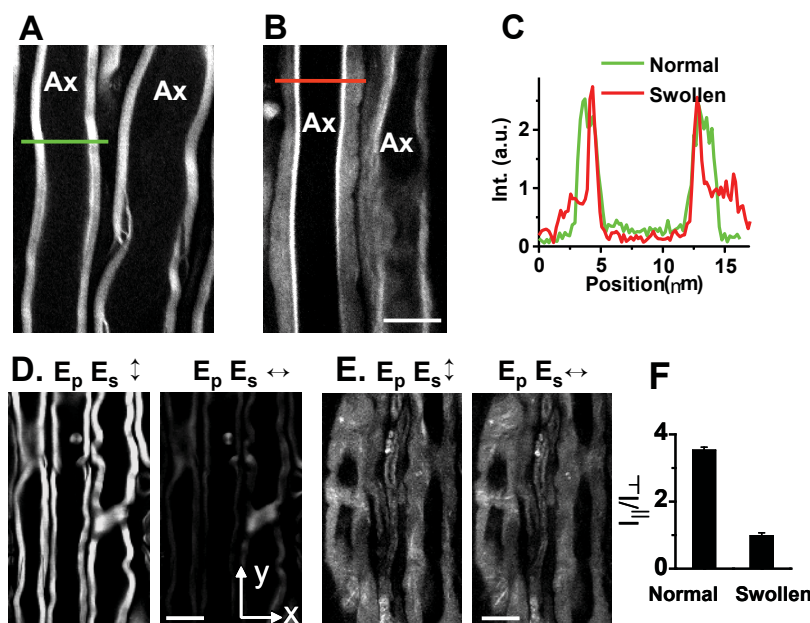


Figure 3. Characterization of lyso-PtdCho induced myelin swelling by CARS microscopy. For all images, bar = 10 μm . (A) CARS image of normal myelin sheath wrapping two parallel axons. (B) CARS image of partially swollen myelin sheath acquired at 5 min after injecting 2 μL of 10 mg/mL lyso-PtdCho into the tissue. (C) CARS intensity profiles of normal and swollen myelin fibers. Green: taken along the green line in (A). Red: taken along the red line in (B). The intensity profiles clearly showed that the CARS intensity from the swollen region was approximately 1/3 of that from the compact region, indicating a reduction of the lipid packing density in the membrane. (D-E) CARS images of normal myelin sheath and totally swollen myelin sheath with vertical (\downarrow) and horizontal (\leftrightarrow) excitation polarization. (F) The ordering degree characterized by I_{\parallel}/I_{\perp} of intra-myelin lipids for normal and swollen myelin sheath. Here I_{\parallel} and I_{\perp} are defined as the CARS intensities with the excitation polarization parallel with or perpendicular to the myelin length. The ratio of I_{\parallel} to I_{\perp} measures the ordering degree of the myelin lipids. For healthy myelin along y-oriented axons (D), the average CARS intensity from the equatorial plane generated with y-polarized beams (I_{\parallel}) is 3.53 (± 0.09) times that with x-polarized beams (I_{\perp}). I_{\parallel} is larger than I_{\perp} because the symmetry axis of the CH₂ groups in the equatorial plane of the myelin is perpendicular to the x direction. For the swollen myelin (E), the value of I_{\parallel}/I_{\perp} was measured to be 0.98 \pm 0.09. Such independence on the excitation polarization ($I_{\parallel} = I_{\perp}$) indicates a complete degradation of the lamellar structure in the swollen myelin sheath.

dimensions were significantly reduced with Ca²⁺ free solution. It was further found that the degradation size was effectively reduced by inhibiting the cPLA₂ or calpain activity. Therefore, the observed acute myelin swelling is largely mediated by Ca²⁺ activated cPLA₂ and calpain.¹⁷

In summary, the capability of imaging intact myelin sheath makes CARS microscopy a unique tool for investigating demyelination mechanism in the ex vivo and in vivo environment, which cannot be performed by traditional methods. In future work, real-time imaging of animal models for multiple sclerosis by combined CARS and TPEF imaging will be performed to clarify the sequence and causality of multiple events (e.g. immune response, damage of oligodendrocyte, release of toxin, demyelination). These studies will contribute to a deeper understanding of the pathology of demyelination diseases.

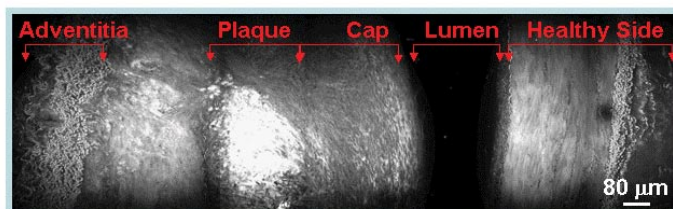


Figure 4. Cross-section CARS image of an iliac artery bearing an atherosclerotic plaque that is enriched in lipids.

4. CARS Imaging of Obesity Associated Health Risks

Obesity is a disorder resulting from the imbalance in energy homeostasis where energy intake exceeds expenditure. When excess energy stored in the form of adipose tissues accumulates such that the body fat mass index rises above 30 kg/m², obesity condition is diagnosed. In the US, obesity has reached an epidemic proportion. According to the Center for Disease Control and Prevention, 66 million American adults are obese.

Being highly sensitive to lipid-rich bio-molecular structures, CARS microscopy serves as an ideal tool for the studies of obesity and associated diseases. At the level of cultured cells, CARS microscopy has been applied to study lipid droplets formation in fibroblast 3T3-L1 cells.¹⁸ Combining CARS and other NLO imaging modalities on the same microscope platform, detailed composition and structural organization of molecular structures within a tissue can be visualized without labeling.¹³ In mammary tumor tissues, CARS allows visualization of adipocytes, tumor cells, and blood capillaries while second harmonic generation imaging allows visualization of collagen fibrils.¹⁹ Intrinsic 3D imaging capability of NLO microscopy enables quantitative analysis of spatial arrangements of such mammary stromal components. In particular, a tumor mass can be readily identified based on the lack of collagen fibrils within the tumor and the abundance of collagen fibrils surrounding the tumor. Additionally, multimodal NLO imaging allows quantitative evaluations of the impacts of obesity on the size of adipocytes in mammary gland and on the collagen fibril content in tumor stroma.¹⁹ Such evaluations are normally inaccessible to standard histological analysis.

Most recently, CARS microscopy has also been applied to visualize molecular composition of arterial walls and atherosclerotic lesions (Fig. 4).^{20, 21} Based on vibrational signals arising from CH₂-rich membrane lipid bilayer, endothelial cells and smooth muscle cells of the arterial walls can be visualized with CARS.²¹ Fibrous protein structures including elastin and collagen can also be visualized with CARS due to the abundance of CH₂ bonds at the cross-linking regions.²¹ Additionally, foam cells rich in lipid droplets and lipid accumulation in the extracellular matrix of an atheroma are readily observable with CARS microscopy.²⁰ To distinguish CARS signals arising from lipid versus those arising from protein, SHG imaging of collagen fibrils and TPEF imaging of elastin are employed simultaneously with CARS imaging.²⁰ Multimodal image acquisition of the same area significantly improves the sensitivity and accuracy in visualizing arterial molecular composition. More importantly, label-free multimodal NLO imaging of atheroma allows identification of areas vulnerable to rupture risks, where there is a significant increase in foam cell accumulation coupled with a drastic reduction in collagen fibrils near arterial lumen.²⁰ Such compositional imaging capability of CARS and other modalities suggests their powerful potential application to the clinical diagnosis of stages of atherosclerotic lesions.

5. Conclusions and Outlook

With chemical selectivity, inherent 3D resolution and capability for high-speed data acquisition, CARS microscopy is poised to become a potent tool for biological imaging. Additionally, the ability to couple CARS with other modalities such as TPEF, SFG and electrophysiological recording provides a powerful multimodal platform to spread the range of applications. Though in this review we have discussed a few areas in which CARS microscopy has shown great promise, the applications for CARS imaging are still in their infancy and will continue to grow for the years to come.

A prohibitive factor in CARS imaging remains the cost and complexity associated with synchronizing two pulsed lasers and effectively coupling them into a scanning microscope. The development of compact, cost-effective laser sources and alternatives to free-space coupling, such as by fiber delivery,²² will

make such a system more attractive to researchers in the biological sciences.

One area in which CARS will prove greatly useful would be *in vivo* imaging of live animals. As magnetic resonance imaging lacks single cell resolution and electron microscopy is incompatible with live tissues, *in vivo* CARS imaging will fill an important niche for study of disease processes. Currently, there are several technical hurdles such as minimizing surgery, compensating for animal motion, and increasing imaging depth which have to be overcome. The development of new technologies such as miniaturization of microscope objective,²³ high-speed scanning,¹⁰ and longer wavelength excitation,⁷ will help to facilitate CARS imaging of live animals.

The demonstrated capability of CARS microscopy in live tissue imaging is expected to stir interests in the development of CARS endoscopy for *in vivo* diagnosis. The advantages of label-free molecular imaging of CARS endoscopy are abundantly obvious. First, label-free imaging overcomes the challenges of inefficient diffusion and non-specific targeting of exogenous fluorophores in the complex *in vivo* environment. Second, because CARS does not require electronic resonance, longer excitation wavelengths can be used to minimize multiphoton absorption induced photodamage. Third, the intrinsic 3D sectioning capability of CARS imaging enables the analysis of spatial organization of bio-structures with molecular details. We anticipate that CARS endoscopy can be coupled with existing imaging modalities such as optical coherence tomography and intravascular ultrasound on the same catheter-based platform. This combination would create a multimodal imaging tool that is capable of 2D morphology mapping with optical coherent tomography and intravascular ultrasound, and 3D sub-micrometric imaging of molecular composition with CARS endoscopy. Such *in vivo* imaging capability would tremendously advance the application of biomedical optics to the diagnosis of cardiovascular diseases.

Acknowledgments

We thank professors Riyi Shi, Ignacio Camarillo, and Michael Sturek for collaborative work on biomedical applications of CARS microscopy. This work is supported by NSF grant 0416785-MCB, NIH grants R21 EB004966 and R01 EB007243.

References

1. Levenson, M. D.; Kano, S. S., Introduction to Nonlinear Laser Spectroscopy. Academic Press: San Diego, 1988.
2. Edidin, M., The state of lipid rafts: from model membranes to cells. *Annu. Rev. Biophys. Biomol. Struct.* 2003, 32, 257-283.
3. Li, L.; Wang, H.; Cheng, J. X., Quantitative coherent anti-Stokes Raman scattering imaging of lipid distribution in co-existing domains. *Biophys. J.* 2005, 89, 3480-3490.
4. Duncan, M. D.; Reintjes, J.; Manuccia, T. J., Scanning coherent anti-Stokes Raman microscope. *Opt. Lett.* 1982, 7, 350-352.
5. Zumbusch, A.; Holtom, G. R.; Xie, X. S., Three-dimensional vibrational imaging by coherent anti-Stokes Raman scattering. *Phys. Rev. Lett.* 1999, 82, 4142-4145.

6. Fu, Y.; Wang, H.; Shi, R.; Cheng, J. X., Characterization of photodamage in coherent anti-Stokes Raman scattering microscopy. *Opt. Express* 2006, 14, 3942-3951.
7. Ganikhanov, F.; Carrasco, S.; Xie, X. S.; Katz, M.; Seitz, W.; Kopf, D., Broadly tunable dual-wavelength light source for coherent anti-Stokes Raman scattering microscopy. *Opt. Lett.* 2006, 31, 1292-1294.
8. Cheng, J. X.; Volkmer, A.; Book, L. D.; Xie, X. S., An epi-detected coherent anti-Stokes Raman scattering (E-CARS) microscope with high spectral resolution and high sensitivity. *J. Phys. Chem. B* 2001, 105, 1277-1280.
9. Volkmer, A.; Cheng, J. X.; Xie, X. S., Vibrational imaging with high sensitivity via epi-detected coherent anti-Stokes Raman scattering microscopy. *Phys. Rev. Lett.* 2001, 87, 023901.
10. Evans, C. L.; Potma, E. O.; Puoris'haag, M.; Côté, D.; Lin, C. P.; Xie, X. S., Chemical imaging of tissue in vivo with video-rate coherent anti-Stokes Raman scattering microscopy. *Proc. Natl. Acad. Sci. USA* 2005, 102, (46), 16807-16812.
11. Huff, T. B.; Cheng, J. X., In vivo coherent anti-Stokes Raman scattering imaging of sciatic nerve tissue. *J. Microsc.* 2007, 225, 190-197.
12. Cheng, J. X.; Jia, Y. K.; Zheng, G.; Xie, X. S., Laser-scanning coherent anti-Stokes Raman scattering microscopy and applications to cell biology. *Biophys. J.* 2002, 83, (1), 502-509.
13. Fu, Y.; Wang, H.; Shi, R.; Cheng, J. X., Second harmonic and sum frequency generation imaging of glial filaments in ex vivo spinal tissues. *Biophys. J.* 2007, 92, 3251-3259.
14. Hirano, A.; Liena, J. F., Morphology of central nervous system axons. In *The Axon Structure, Function and Pathophysiology*, Waxman, S. G.; Kocsis, J. D.; Stys, P. K., Eds. Oxford University Press: New York, 1995; pp 49-67.
15. Wang, H.; Fu, Y.; Zickmund, P.; Shi, R.; Cheng, J. X., Coherent anti-Stokes Raman scattering imaging of axonal myelin in live spinal tissues. *Biophys. J.* 2005, 89, 581-591.
16. Blakemore, W. F.; Eames, R. A.; Smith, K. J.; McDonald, W. I., Remyelination in the spinal cord of the cat following intraspinal injections of lysolecithin. *J. Neurol. Sci.* 1977, 33, (1-2), 31-43.
17. Fu, Y.; Wang, H.; Huff, T. B.; Shi, R.; Cheng, J. X., Coherent anti-Stokes Raman scattering imaging of myelin degradation reveals a calcium dependent pathway in lyso-PtdCho induced demyelination. *J. Neurosci. Res.*, in press, 2007.
18. Nan, X.; Cheng, J. X.; Xie, X. S., Vibrational imaging of lipid droplets in live fibroblast cells using coherent anti-Stokes Raman microscopy. *J. Lipid Res.* 2003, 40, 2202-2208.
19. Le, T. T.; Rehrer, C. R.; Huff, T. B.; Nichols, M. B.; Camarillo, I. G.; Cheng, J. X., Nonlinear optical imaging to evaluate the impact of obesity on mammary gland and tumor stroma. *Mol. Imaging*, 2007, 6, 205-211.
20. Le, T. T.; Langohr, I. M.; Locker, M. J.; Sturek, M.; Cheng, J. X., Label-free molecular imaging of atherosclerotic lesions with multi-modal nonlinear optical microscopy. *J. Biomed. Opt.*, in press, 2007.
21. Wang, H. W.; Le, T. T.; Cheng, J. X., Label-free imaging of arterial cells and extracellular matrix using a multimodal nonlinear optical microscope. *Opt. Comm.* in press, 2007.
22. Wang, H.; Huff, T. B.; Cheng, J. X., Coherent anti-Stokes Raman scattering imaging with a laser source delivered by a photonic crystal fiber. *Opt. Lett.* 2006, 31, 1417-1419.
23. Wang, H.; Huff, T. B.; Fu, Y.; Jia, K. Y.; Cheng, J. X., Increasing the imaging depth of coherent anti-Stokes Raman scattering microscopy with a miniature microscope objective. *Opt. Lett.* 2007, 32, 2212-2214.

About the Authors



Ji-Xin Cheng was born in Jixi, Anhui, China. He received his B.S. and Ph D from University of Science and Technology of China in 1998. After being a postdoctoral fellow at Harvard University, he joined the faculty of Weldon School of Biomedical Engineering at Purdue University in 2003. His research interests include cell biophysics, nonlinear optical imaging, and nanomedicine development.

Haifeng Wang received his B.S. in 1998 from Tsinghua University, Beijing, China and his Ph.D. in 2003 from the School of Electrical and Computer Engineering, Purdue University, West Lafayette, IN. Since 2004 he has been a postdoctoral fellow at the Weldon School of Biomedical Engineering, Purdue University. Thuc T. Le received his B.A. from the University of California, Berkeley in 1998 and his Ph.D. from the University of Chicago in 2005. He is currently a Ruth L. Kirschstein post-doctoral fellow at the Weldon School of Biomedical Engineering at Purdue University.

Yan Fu received her B.S. and M.S. from Tsinghua University, Beijing of China in 2000 and 2003, respectively. She is currently a Ph.D. candidate in Dr. Ji-Xin Cheng's group at the Weldon School of biomedical Engineering at Purdue University. Terry B. Huff received his B.S. from the University of Central Oklahoma in 2004. He is currently a Ph.D. candidate in Dr. Ji-Xin Cheng's group in the Department of Chemistry at Purdue University. Han-Wei Wang received his B.S. and M.S. degrees in mechanical engineering from National Tsing Hua University, Hsinchu, Taiwan, in 2000 and 2002 respectively. From 2002 to 2006 he was an R&D Engineer in DR. Chip Biotechnology Incorporation in Taiwan. Currently he is a doctoral student in Dr. Ji-Xin Cheng's group at the Weldon School of Biomedical Engineering at Purdue University.